A Smooth-Turn Mobility Model for Airborne Networks

Yan Wan, *Member, IEEE*, Kamesh Namuduri, *Senior Member, IEEE*, Yi Zhou, *Student Member, IEEE*, and Shengli Fu, *Senior Member, IEEE*

***Abstract*—The design of effective routing protocols in airborne networks (ANs) relies on suitable mobility models that capture the movement patterns of airborne vehicles. As airborne vehicles cannot make sharp turns as easily as ground vehicles do, the widely used ground-based mobile ad hoc network (MANET) mobility models are not appropriate to use as the analytical frameworks for airborne networking. In this paper, we introduce a novel mobility model, which is called the smooth-turn (ST) mobility model, that captures the correlation of acceleration of airborne vehicles across temporal and spatial coordinates. The proposed model is realistic in capturing the tendency of airborne vehicles toward making straight trajectories and STs with large radii, yet is tractable enough for analysis and design. We first describe the mathematics of this model and then prove that the stationary node distribution is uniform. Furthermore, we introduce a metric to quantify the degree of model randomness, and using this, we compare and classify several mobility models in the literature. We conclude this paper with several possible variations to the basic ST mobility model.**

***Index Terms*—Airborne networks, mobility models, randomness.**

I. Introduction

THE WIDE variety of military and civilian applications of airborne networking have resulted in dramatically growing research effort in airborne networks (ANs) over the past few years. Supported by the advances in sensing and wireless communication technologies, ANs hold promise in providing effective, widely applicable, low-cost, and secure information exchange among airborne vehicles. For instance, the in-flight communication among commercial airlines can allow the sharing of adverse weather conditions and emergencies, which are of significant value, particularly when the flights are in areas outside the reach of ground control stations. Similarly, unmanned airborne vehicles (UAVs) may rely on fast communication and networking schemes for safe maneuvering. It is anticipated that ANs will be the platform for information exchange among airborne vehicles and connect with space and ground networks to complete the future multiple-domain communication networks [38], [40].

In the study of ANs, significant effort has been focused on the development of reliable routing protocols that minimize the number of packets that is lost due to link and path failures [16], [24], [32], [35], [37], [40]. Designing robust routing strategies is challenging, considering the unique attributes of ANs such as high node mobility and frequent topology changes. For example, several widely used routing algorithms that are based on the principle of the shortest path tend to find paths with relay nodes at the edges of transmission radius [27], leading to what is known as "edge effect." In such a scenario, even a slight movement of nodes can lead to link failures. This edge effect prominently occurs in highly varying networks such as ANs. Therefore, we anticipate that designing reliable routing strategies with minimal impact of edge effect should take into account the statistically varying AN structure. The statistics of interest include node distribution, movement, connectivity patterns, etc. [12].

Mobility models commonly serve as the fundamental mathematical framework for network connectivity analysis, network performance evaluation, and, eventually, the design of reliable routing protocols [17]. In particular, mobility models capture the random movement pattern of each network agent, based on which rich information related to the varying network structure can be derived, such as node distribution, link statistics, and path lifetime. Some mobility models have been extensively studied in the literature; the most well-known among them include random direction (RD) and random waypoint (RWP) [5], [8], [11], [22]. The RWP model assumes that an agent chooses a random destination (waypoint) and traveling speed. Upon reaching the waypoint, it pauses, and then travels to the next waypoint. The basic RD model assumes that nodes travel between endpoints located at region boundaries [21]. The extended version allows an agent to randomly select a speed and direction after the completion of a randomly chosen traveling time [18], [19]. The stochastic properties of these common models, such as their spatial distributions, can be found in, e.g., [5], [8], [11], [22], and [31].

Developing suitable mobility models for ANs is undoubtedly the foundation for designing realistic AN networking strategies. We note that the widely used RWP and RD models are well suited to describe the random activity of mobile nodes in mobile ad hoc networks (MANETs); however, they lack the ability to capture the unique features of airborne mobility. In particular, mobile nodes on the ground can easily slow down, make sharp turns, and travel in an opposite direction

Manuscript received July 11, 2012; revised December 4, 2012; accepted January 31, 2013. Date of publication March 7, 2013; date of current version September 11, 2013. The work of Y. Wan was supported by the National Science Foundation under Grant 1035386 and Grant 1058110. This paper was presented in part at the First ACM MobiHoc Workshop on Airborne Networks and Communications, Hilton Head Island, SC, USA, June 11–14, 2012. The review of this paper was coordinated by Prof. Y.-B. Lin.

The authors are with the Department of Electrical Engineering, University of North Texas, Denton, TX 76203 USA (e-mail: yan.wan@unt.edu).

Color versions of one or more of the figures in this paper are available online at http://ieeexplore.ieee.org.

Digital Object Identifier 10.1109/TVT.2013.2251686

(see an enhanced random mobility model that captures such movement [6]). However, airborne vehicles tend to maintain the same heading speed and change direction through making turns with large radii. This unique feature is caused by the mechanical and aerodynamic constraints for airborne vehicles and reflected in the *correlation in acceleration along spatial* and *temporal dimensions*. Our aim here is to develop *realistic* models that capture such features unique to ANs yet are *simple* and *tractable* enough to facilitate connectivity analysis and routing design.

Let us relate our modeling effort with the very limited existing AN mobility models [36], [40], [44]. We believe that AN mobility models need to be *application specific* because of their wide variety of applications and the associated different movement patterns. Within this framework, let us summarize three types of AN models in the literature, including our proposed model, by focusing on specific applications and the movement patterns associated with each application.

1) SRCM Mobility Model for Search and Rescue Applications: In this model, each UAV moves around a fixed center with a randomly selected radius; after it completes a round, it chooses another radius and circles around the *same* center [44]. Although this model seems to be limited as the movement is constrained by the location of the fixed circling center, it captures well the mobility of UAVs in *search* and *rescue* applications, in which the potential location of a search target is usually available and chosen as the fixed center, and UAVs are dispatched to hover around the center to pinpoint the exact target location. The knowledge about the potential target location (used as the fixed center) provides extra information for predicting trajectories and connectivity structures of the AN.

2) FP-Based Mobility Model for Cargo and Transportation Applications: In this mobility model, a mobility file is created using the predefined flight plan (FP) and is then converted into a time-dependent network topology (TDNT) map for the design and update of routing protocols [40]. If the actual flight status deviates from the predescribed plan, the TDNT and the relevant routes are updated. The FP-based model is well suited for *cargo* and *transportation* purposes, in which the entire trajectory is usually planned in advance. Although various *uncertainties* such as weather events, departure delays, etc., may effect the adherence to the FPs [42], [43], the existence of a plan allows for a more accurate prediction of flight trajectories and, hence, the varying network topology beforehand [9], [45]. The ground station (GS) mode of the AeroRP protocol [32] is similar in the sense that the GS periodically broadcasts the update of AN topology, and also when a change in topology is sensed.

3) ST Mobility Model for Patrolling Applications: The given two AN mobility models assume the availability of abundant trajectory information. However, in AN applications such as *patrolling*, a predefined trajectory or a potential target location might not be available; instead, airborne vehicles simply *swarm* in a certain defined region in the airspace. Such flexible movement resembles the highly random RD model for MANETs. In this paper, we present a novel mobility model called the smooth-turn (ST) mobility model, which allows *flexible* trajectories while also taking into account the features unique to airborne vehicles, e.g., the preference toward *smooth* rather than sharp turns. Capturing such ST features in mobility models can better represent realistic maneuvering of airborne vehicles and improve the capability of path estimation and connectivity analysis for ANs. This new model is realistic in capturing the random movement of airborne vehicles in favor of STs, yet is *analyzable* for node distribution and connectivity analysis. We note that Gauss–Markov models (as described in [5], [26], and [36]) may also be suited for patrolling applications, as they describe the memory-equipped movement of airborne vehicles. However, as we will discuss in Section II-B, which was also presented in [25] and [30], these models may not directly capture the kinematics of *turning* aerial objects.

Our paper contributes to the existing literature on mobility models in the following ways.

- *A novel AN mobility model that captures STs*: This mobility model resembles the traditional RD model in terms of the flexibility of trajectories but captures the temporal and spatial correlation specific to the movement of airborne vehicles. The model is well suited for patrolling applications, in complementary to limited existing AN models in the literature. In addition, a significant feature of the model is that it is simple enough to serve as the framework not only for simulation studies but for tractable theoretical analysis as well.
- *The stationary analysis and preliminary connectivity analysis of the model*: We prove that the stationary node distribution of this ST model is *uniform*. The nice uniformity directly leads to a series of closed-form results for connectivity.
- *A metric to quantify the degree of randomness for mobility models*: We envision that the formal analysis of trajectory *predictability/randomness* can help better understand the difference and applicability of AN (and more general) mobility models and, more importantly, help design smart predictability-based routing algorithms. As such, we introduce a metric to quantify the randomness of future trajectory using the concept of *entropy* and compute this metric for four mobility models.
- *The classification* and *comparison of different types of AN mobility models*: We identify the need to use different mobility models for different applications and group AN mobility models according to application categories and entropy-based randomness levels.

This paper is organized as follows. In Section II, we describe the ST mobility model and present the basic analysis of its dynamics. In Section III, we investigate the stationary distribution of the model using theoretical analysis and simulations. In Section IV, we motivate and formulate the concept of predictability/randomness, and provide a comparison of our model with three other mobility models in the literature, in terms of the degree of randomness. In Section V, multiple variants and enhanced versions of the ST mobility model are discussed and simulated. Finally, a brief conclusion and discussion about future works are provided in Section VI.

II. Smooth-Turn Mobility Model

Here, we first describe the basic mathematical ST mobility model in Section II-A. We then discuss the roles of model parameters and relate the model with relevant models in the literature in Section II-B. We also describe the models by capturing how nodes move at boundaries. Finally, in Section II-C, we present the basic analysis of the model dynamics.

A. Basic Model Description

We introduce the ST mobility model to capture the movement of airborne vehicles in highly random ANs. The model captures the unique feature of airborne vehicles, i.e., the strong spatiotemporal correlation of acceleration. Incorporating this special feature into mobility models increases the predictability of a vehicle's trajectory, which in turn facilitates connectivity analysis and the design of networking strategies.

The idea behind the ST random mobility model is simple. An airborne vehicle selects a point in the space along the line *perpendicular* to its heading direction and circles around it until the vehicle chooses another turning center. This perpendicularity ensures smooth flight trajectories. In addition to that, we assume the waiting time for the change of turning centers to be *memoryless*, i.e., the timing of the center change does not depend on the duration for which the UAV has maintained its current center. This memoryless model is typically used to abstract the waiting time for the occurrence of random events as it brings in the nice tractability of renewable processes [33]. For instance, connectivity analysis can be taken at any time instance without prior knowledge of how long a vehicle has kept its current mobility status. Furthermore, since a vehicle commonly favors straight trajectories and slight turns than very sharp turns, we model the inverse length of the turning radius to be Gaussian distributed.

Now, let us describe the mathematics of the model. We use $l_x(t)$, $l_y(t)$, $v_x(t)$, $v_y(t)$, $w(t)$, and $\Phi(t)$ to denote the x and y coordinates, velocities in x-direction and y-direction, angular velocity, and the heading angle at time t, respectively. For simplicity and realistic considerations, we assume a constant forward speed V in a 2-D plane; therefore, the tangential acceleration $a_t(t)$ is 0 [see (1)]. This assumption is reasonable for airborne vehicles, particularly for jets and gliders, as they tend to maintain the same speed in flight and "reduce speed" through zigzagging and circling [3].

Furthermore, the vehicle changes its centripetal acceleration $a_n(t)$ at randomly selected time points T_0, T_1, $T_2, \ldots$, where $0 = T_0 < T_1 < T_2 < \cdots$. The duration for the vehicle to maintain its current centripetal acceleration $\tau(T_i) = T_{i+1} - T_i$ follows exponential distribution as motivated by its memoryless property [33]. In particular, the probability density function $f(\tau(T_i)) = \lambda e^{-\lambda \tau(T_i)}$, where $1/\lambda$ is the mean of $\tau(T_i)$.

Next, we describe how the new centripetal acceleration $a_n(t)$ is selected at each time point T_i. $a_n(T_i)$ is determined by the randomly selected turning radius $r(T_i)$ according to $a_n(T_i) = V^2/r(T_i)$ [see (2)]. The selection of $r(T_i)$, i.e., the distance between the vehicle's current location $(l_x(T_i), l_y(T_i))$, also determines the new turning center with coordinates $(c_x(T_i)), c_y(T_i))$ (see Fig. 1(b) and the details in Section II-C). It is important to note that the new turning center $(c_x(T_i)), c_y(T_i))$ resides along the line perpendicular to the heading of the vehicle at time T_i (denoted by $\Phi(T_i)$), to guarantee smoothness. In addition, it is worth noting that random variable $r(T_i) \in R$ allows turns to both left and right, with $r(T_i) > 0$ representing the right turns. $1/r(T_i)$ is a Gaussian random variable with zero mean and variance σ^2. This distribution is selected so that straight trajectories and large-radius turns are favorable than sharp turns with small radii.

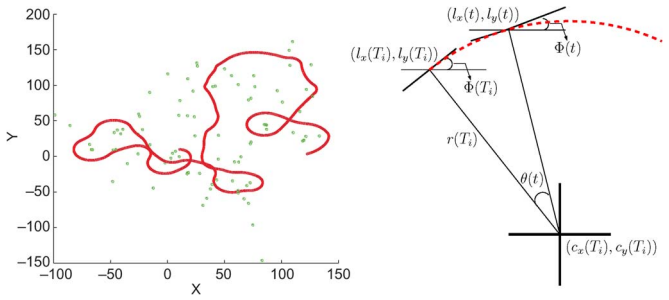

Fig. 1. (a) Simulation of the trajectory (red curve) of an UAV in a 2-D domain. Green spots are the randomly chosen turning centers. (b) Trajectory analysis diagram to predict the location of an airborne vehicle at any $T_{i+1} \geq t \geq T_i$. The dashed red curve represents the trajectory.

Finally, (3)–(5) describe the relationships among location, heading angle, velocity, and angular velocity (see [25] for a review of dynamic models for moving aerial objects). In summary, the dynamics of the basic ST mobility model during the time interval $T_i \leq t < T_{i+1}$ is shown in the following:

$$a_t(t) = 0 \tag{1}$$

$$a_n(t) = \frac{V^2}{r(T_i)} \tag{2}$$

$$\dot{\Phi}(t) = -w(t) = -\frac{V}{r(T_i)} \tag{3}$$

$$\dot{l}_x(t) = v_x(t) = V\cos(\Phi(t)) \tag{4}$$

$$\dot{l}_y(t) = v_y(t) = V\sin(\Phi(t)) \tag{5}$$

where the "$\cdot$" symbol represents the first-order derivative with respect to time. Because a vehicle keeps its centripetal acceleration for a duration of $\tau(T_i)$ before changing its centripetal acceleration, it is easy to see that, during the interval, $T_i \leq t < T_{i+1}$, $r(t) = r(T_i)$, $a_n(t) = a_n(T_i)$, $c_x(t) = c_x(T_i)$, $c_y(t) = c_y(T_i)$, and $\tau(t) = \tau(T_i)$. A typical trajectory of the model is shown in Fig. 1. The simulation is written in MATLAB, and the code is available in [1].

B. Further Discussions of the Model

The ST mobility model naturally captures the highly random movement patterns of ANs, and the preference toward straight trajectories and large STs with constant speed and turn rate. Here, let us first comment on the three parameters in the model and then connect the model with the RD model and target-tracking models. Finally, we discuss two models capturing the movement at boundaries.

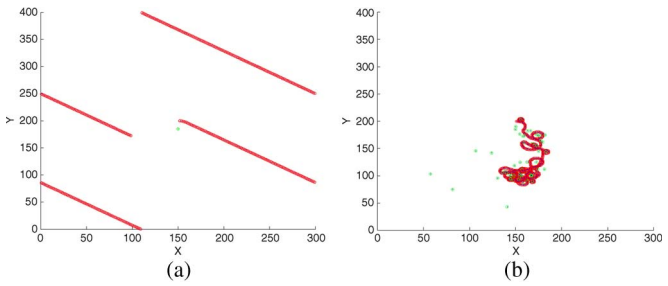

Fig. 2. Simulations of the ST mobility model to show the impact of parameters on the trajectories. (a) When σ^2 is close to 0. (b) When σ^2 and λ are large, and the ratio between V and the two given is also large.

The first parameter is the vehicle speed V. ANs typically have high vehicle speed (in the range of 50–500 mi/h or more), which causes highly varying connectivity structures. The second parameter is the inverse of the mean of the exponential random variable $\tau(T_i)$, i.e., λ. A large λ indicates that the airborne vehicle frequently changes its turning center and thus results in a more wavy trajectory. The last parameter is the variance of the Gaussian variable $1/r(T_i)$, i.e., σ^2, which determines the preference for straight trajectory versus turns. In particular, a small variance denotes the high possibility of a very large turning radius and, therefore, a more straight trajectory. At one extreme, if the variance is close to 0, the ST mobility model has very straight trajectories, which resemble those of the RD model without a directional change, as shown in Fig. 2(a). At the other extreme, a large σ^2, large V, and large λ result in more curvy trajectories [see Fig. 2(b)]. Through choosing proper combinations of the parameters V, λ, and σ^2, the model can capture a wide range of AN mobility patterns.

It is worthwhile to relate our ST mobility model with two relevant categories of models in the literature. First, we can view the ST model as an *RD model equipped with a smooth trajectory* because of their similarities. In the RD model, an agent chooses a random *straight direction* and follows it before choosing the next direction. Similarly, in the ST model, an agent chooses a random *turning center* and circles around it before choosing the next center. We will see in Section II-C that the node distribution of our model also resembles that of the RD. Second, our model is built upon the abundant literature in the context of aerial target tracking (see e.g., [25] for a thorough review). Let us briefly discuss the works in this field as they thoroughly studied the kinematics of aerial objects and laid out the theoretical foundation for our model. Early models in this field assume that the acceleration is *uncorrelated* in 2-D or 3-D space, and abstract acceleration in each coordinate is assumed as a Markov process (e.g., random noise passing through a linear system) [20], [25], [39]. The Gauss–Markov model adopted in [36] is an extension of these works. The latter models, which are known as the *coordinated turn models*, reflect the *physical laws* of airborne objects (see e.g., [25] and [30]) and, therefore, better capture the correlation of acceleration among coordinates. However, because these models are built for target-tracking purposes, they focus on the high-precision prediction of the acceleration and path of an individual aircraft; therefore, their motion dynamics are more complex than necessary for our purpose. We capture the correlation

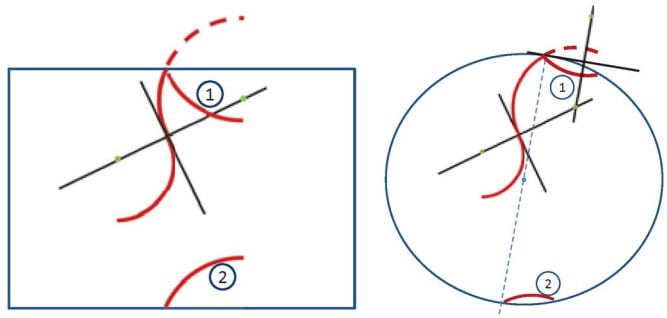

Fig. 3. (a) Reflection (1) and the wrap-around (2) boundary models in a rectangular region. (b) Reflection (1) and the wrap-around (2) models in a circular region. Red bold curves represent the real trajectories.

across spatiotemporal coordinates through a simple parameter, i.e., the turning radius r, making the model at a coarse *statistical-group level* and simple enough for mobility analysis.

Another topic to discuss is the modeling of node movements at boundaries. In this paper, we adopt the boundary models typically used for the RD model, namely the "wrap-around" and the "reflection" models [7], [31]. In the "wrap-around" model, after an airborne vehicle hits the boundary, it wraps around and appears at the opposite side of the region. Alternatively, in the "reflection" model, the trajectory is mirrored against that boundary. Typical trajectories of these two boundary models are shown in Fig. 3. Although these movement patterns may not be typical in reality, they provide rich analyzability and permit us to focus more on the mobility itself instead of the impact of boundaries. In the rest of this paper, we largely focus on the "wrap-around" model but will also briefly discuss the "reflection" model.

C. Basic Model Analysis

We consider an airborne vehicle flying within a rectangular airspace $[0, L] \times [0, W]$. Assuming the wrap-around boundary model, the mobility state of the vehicle at any $T_i \le t < T_{i+1}$ can be obtained from the state at time T_i, as shown in the following:

$$c_x(T_i) = l_x(T_i) + r(T_i)\sin(\Phi(T_i)) \tag{6}$$

$$c_y(T_i) = l_y(T_i) - r(T_i)\cos(\Phi(T_i)) \tag{7}$$

$$\theta(t) = \frac{V}{r(T_i)}(t - T_i) \tag{8}$$

$$\Phi(t) = \Phi(T_i) - \theta(t) - 2\pi\left\lfloor \frac{\Phi(T_i) - \theta(t)}{2\pi} \right\rfloor \tag{9}$$

$$l_x(t) = c_x(T_i) - r(T_i)\sin(\Phi(t)) - W\left\lfloor \frac{c_x(T_i) - r(T_i)\sin(\Phi(t))}{W} \right\rfloor \tag{10}$$

$$l_y(t) = c_y(T_i) + r(T_i)\cos(\Phi(t)) - L\left\lfloor \frac{c_y(T_i) - r(T_i)\cos(\Phi(t))}{L} \right\rfloor. \tag{11}$$

These equations can be easily derived from (1)–(5) by observing the relationship between node locations and the turning center, as shown in Fig. 1(b). In particular, as the turning center

is along the line perpendicular to the heading direction, its x and y locations $c_x(T_i)$ and $c_y(T_i)$, respectively, can be expressed in terms of node locations at time T_i using the trigonometric functions, as shown in (6) and (7). The turning angle $\theta(t)$ is the difference between $\Phi(T_i)$ and $\Phi(t)$. As velocity V is fixed, $\theta(t)$ is equal to the arc length divided by the turning radius $r(T_i)$, as shown in (8). The floor function (denoted by "$\lfloor\rfloor$") in (9) guarantees that $\Phi(t)$ is within 0 and 2π (see [31] for the detailed illustration). Once the heading direction at time t, i.e., $\Phi(t)$, is calculated, the node location at time t can be expressed in terms of the turning center, again using trigonometric functions [see (10) and (11)]. Similar to (9), these floor functions implement the wrap-around boundary model: If the location is beyond (W, L) by (w, l), it is shifted to (w, l).

With regard to the reflection boundary model, the only changes are to replace (10) and (11) with

$$\begin{aligned} l_x(t) =& c_x(T_i) - r(T_i)\sin(\Phi(t)) \\ & - 2W\left\lfloor \frac{c_x(T_i) - r(T_i)\sin(\Phi(t))}{2W} + \frac{1}{2} \right\rfloor \quad (12) \\ l_y(t) =& c_y(T_i) + r(T_i)\cos(\Phi(t)) \\ & - 2L\left\lfloor \frac{c_y(T_i) - r(T_i)\cos(\Phi(t))}{2L} + \frac{1}{2} \right\rfloor. \quad (13) \end{aligned}$$

The floor functions and the addition of 0.5 guarantee that the trajectory is reflected back into the region when an agent moves to the boundary (as motivated by triangular wave forms [2]). The given motion analysis [see (6)–(13)] will be used to derive a variety of properties of the ST mobility model in the rest of this paper.

III. Node Distribution and Connectivity

Here, we consider multiple airborne vehicles following the ST mobility model. We analyze the distribution of node locations and heading angles in Section III-A. The analysis is based upon that of the RD model [31], but here, it is based upon that of the mobility model with smooth trajectory. The uniform node distribution gives rise to interesting properties in terms of network connectivity, which we will briefly summarize.

A. Node Distribution

Lemma 1: $\int_{u=0}^{b} \mathbf{1}\{u+a-b\lfloor (u+a)/b\rfloor < x\}du = x$ holds for any $x \in [0, b]$, where $a \in R$, $b \in R^+$, and $\mathbf{1}\{\}$ is 1 if $\{\}$ is true and 0 if $\{\}$ is false.

Proof: Introduce $u' = u/b$. According to the property of floor operations [31], we have

$$\begin{aligned} & \int_{u=0}^{b} \mathbf{1}\left\{u + a - b\left\lfloor \frac{u+a}{b} \right\rfloor < x\right\} du \\ & = b\int_{u'=0}^{1} \mathbf{1}\left\{u' + \frac{a}{b} - \left\lfloor u' + \frac{a}{b} \right\rfloor < \frac{x}{b}\right\} du' = b\frac{x}{b} = x. \quad (14) \end{aligned}$$

Theorem 1: N airborne vehicles independently move in the space $[0, L) \times [0, W)$ according to the ST mobility model associated with the wrap-around boundary model. If the initial locations of these vehicles are uniformly distributed in $[0, L] \times [0, W]$ and the heading angles are also initially uniformly distributed in $[0, 2\pi)$, then the node locations and heading angles remain uniformly distributed for any $t > 0$.

Proof: Let us first examine a single vehicle and show that, if its position and heading angle are uniformly distributed initially, they remain uniformly distributed. Then, because the vehicles independently move, we can show the uniform distribution of node locations and heading angles for all vehicles.

For a moment, we consider the fixed movement pattern of a vehicle. In particular, the time sequence to change the turning center $0 = T_0 \le T_1 \le T_2, \ldots$ and the corresponding radii $r(T_0)$, i.e., $r(T_1), \ldots$, are all fixed. Let us show that, for each fixed movement pattern, uniform distribution remains for any $t > 0$.

We start with examining any time $t \in [T_0, T_1)$. At initial time T_0, the joint probability distribution function (pdf) satisfies $P(l_x(T_0) < x_0, l_y(T_0) < y_0, \Phi(T_0) < \Phi_0) = (x_0/L)(y_0/W)(\Phi_0/2\pi)$ for any $0 \le x_0 < L$, $0 \le y_0 < W$, and $0 \le \Phi < 2\pi$. Let us prove that $P(l_x(t) < x,\ l_y(t) < y,$ and $\Phi(t) < \Phi) = (x/L)(y/W)(\Phi/2\pi)$ for any $0 \le x < L,\ 0 \le y < W,$ and $0 \le \Phi < 2\pi$.

Equations (6)–(11) indicate that $l_x(t)$, $l_y(t)$, and $\Phi(t)$ are functions of $l_x(T_0)$, $l_y(T_0)$, $\Phi(T_0)$, $r(T_0)$, and T_0 as follows:

$$\begin{aligned} \Phi(t) =& \Phi(T_0) - \frac{V}{r(T_0)}(t - T_0) - 2\pi\left\lfloor \frac{\Phi(T_0) - \frac{V}{r(T_0)}(t-T_0)}{2\pi} \right\rfloor \\ l_x(t) =& l_x(T_0) + r(T_0)\sin(\Phi(T_0)) - r(T_0)\sin(\Phi(t)) \\ & - W\left\lfloor \frac{l_x(T_0) + r(T_0)\sin(\Phi(T_0)) - r(T_0)\sin(\Phi(t))}{W} \right\rfloor \\ l_y(t) =& l_y(T_0) - r(T_0)\cos(\Phi(T_0)) + r(T_0)\cos(\Phi(t)) \\ & - L\left\lfloor \frac{l_y(T_0) - r(T_0)\cos(\Phi(T_0)) + r(T_0)\cos(\Phi(t))}{L} \right\rfloor. \end{aligned} \quad (15)$$

For the convenience of presentation, we denote the expressions in the right of the given three equations as $\Psi(\Phi(T_0), r(T_0), t, T_0)$, $\Lambda_x(l_x(T_0), \Phi(T_0), r(T_0), t, T_0)$, and $\Lambda_y(l_y(T_0), \Phi(T_0), r(T_0), t, T_0)$, respectively. Using the abbreviated notations and according to (15), we can find the joint pdf of $P(l_x(t) < x, l_y(t) < y, \Phi(t) < \Phi)$ as

$$\begin{aligned} & P(l_x(t) < x, l_y(t) < y, \Phi(t) < \Phi) \\ & \quad = P\left(\Lambda_x(l_x(T_0), \Phi(T_0), r(T_0), t, T_0) < x\right. \\ & \Lambda_y\left(l_y(T_0), \Phi(T_0), r(T_0), t, T_0\right) < y \\ & \quad \left.\Psi\left(\Phi(T_0), r(T_0), t, T_0\right) < \Phi\right) \\ & \quad = \int_{\Phi(T_0)=0}^{2\pi} \frac{1}{2\pi} \int_{l_x(T_0)=0}^{L} \frac{1}{L} \int_{l_y(T_0)=0}^{W} \frac{1}{W} \\ & \mathbf{1}\left\{\Psi\left(\Phi(T_0), r(T_0), t, T_0\right) < \Phi\right\} \\ & \quad \times \mathbf{1}\left\{\Lambda_x\left(l_x(T_0), \Phi(T_0), r(T_0), t, T_0\right) < x\right\} \\ & \mathbf{1}\left\{\Lambda_y\left(l_y(T_0), \Phi(T_0), r(T_0), t, T_0\right) < y\right\} \\ & \quad \times dl_x(T_0)dl_y(T_0)d\Phi(T_0) \end{aligned}$$

$$= \frac{1}{2\pi WL} \int_{\Phi(T_0)=0}^{2\pi} \mathbf{1}\left\{\Psi\left(\Phi(T_0), r(T_0), t, T_0\right) < \Phi\right\} \int_{l_x(T_0)=0}^{W} \mathbf{1}\left\{\Lambda_x\left(l_x(T_0), \Phi(T_0), r(T_0), t, T_0\right) < x\right\} dl_x(T_0) \int_{l_y(T_0)=0}^{L} \left\{\Lambda_y\left(l_y(T_0), \Phi(T_0), r(T_0), t, T_0\right) < y\right\} dl_y(T_0) d\Phi(T_0). \tag{16}$$

The last equality is due to the independence of l_x and l_y.

According to Lemma 1, we can easily see that $\int_{l_x(T_0)=0}^{W} \mathbf{1}\{\Lambda_x(l_x(T_0), \Phi(T_0), r(T_0), t, T_0) < x\} dl_x(T_0) = x$. A similar relationship holds for l_y. As such, (16) is further simplified to

$$P\left(l_x(t) < x, l_y(t) < y, \Phi(t) < \Phi\right) = \frac{xy}{2\pi WL} \int_{\Phi(T_0)=0}^{2\pi} \mathbf{1}\left\{\Psi\left(\Phi(T_0), r(T_0), t, T_0\right) < \Phi\right\} d\Phi(T_0) = \frac{x}{L}\frac{y}{W}\frac{\Phi}{2\pi}. \tag{17}$$

The given proof shows that the uniform distribution remains in the time interval $[T_0, T_1)$ for a particular movement pattern. Furthermore, let us denote the time right before t as t^-. We then easily observe that $\Phi(T_1) = \Phi(T_1^-)$ because choosing a new center $(c_x(T_1), c_y(T_1))$ along the line perpendicular to the heading angle $\Phi(T_1^-)$ at time T_1 does not change the heading angle at T_1. Combining the facts that $l_x(T_1) = l_x(T_1^-)$ and that $l_y(T_1) = l_y(T_1^-)$, we conclude that the uniform distribution also holds for the closed time interval $[T_0, T_1]$.

The proof to show that the uniform distribution remains during $[T_1, T_2]$ and any $[T_i, T_{i+1}]$ follows exactly the same procedure. Therefore, uniform distribution remains for any time $t \geq 0$ for each particular movement pattern and, therefore, generally for a particular vehicle.

Because the N vehicles independently move, the joint distribution of node locations and heading angles is the multiplication of individual distributions. As each individual distribution is uniform, we can conclude that the N vehicles' node locations and heading angles remain uniformly distributed at any time $t \geq 0$. The proof is complete.

Theorem 1 informs that the uniform distribution at the initial time is preserved. The next theorem says that the steady-state distribution is uniform, independent from the initial distribution.

Theorem 2: N airborne vehicles independently move in the space $[0, L] \times [0, W]$ according to the ST mobility model associated with wrap-around boundary model. Assuming that λ and σ are finite and not equal to 0, the distributions of node locations and heading angles are uniform in $[0, L) \times [0, W)$ and $[0, 2\pi)$, respectively, in the limit of large time, regardless of the distribution at the initial time.

Proof: Let us first sketch the structure of the proof. We first construct a Markov process with states $S(t) = (l_x(t), l_y(t), \Phi(t), (1/r)(t), \tau(t))$ and find the probability transition kernel for the Markov chain defined at the time sequence T_i, namely $S(T_i)$. We then find the invariant distribution of $S(T_i)$. The Palm Formula [4], [31] is then used to find the limiting probability distribution of the Markov process $S(t)$.

First, we note that $S(t)$ is a Markov process because $S(t + \Delta t)$ is only dependent upon $S(t)$ but not on any state before time t. $S(T_i)$ for $i = 0, 1, \ldots$ form a discrete-time Markov chain, with the following transition probability kernel:

$$\begin{aligned} &f(S(T_{i+1})|S(T_i)) \\ &\quad = f\left(l_x(T_{i+1}) = \Lambda_x(l_x(T_i), \Phi(T_i), r(T_i), T_{i+1}, T_i)\right. \\ &l_y(T_{i+1}) \\ &\quad = \Lambda_y\left(l_y(T_i), \Phi(T_i), r(T_i), T_{i+1}, T_i\right) \\ &\Phi(T_{i+1}) \\ &\quad = \Psi\left(\Phi(T_i), r(T_i), T_{i+1}, T_i\right), \frac{1}{r}(T_{i+1}), \tau(T_{i+1})|l_x(T_i) \\ &l_y(T_i), \Phi(T_i), \frac{1}{r}(T_i), \tau(T_i)) \\ &\quad = \mathbf{1}\left\{l_x(T_{i+1}) = \Lambda_x\left(l_x(T_i), \Phi(T_i), r(T_i), T_{i+1}, T_i\right)\right\} \\ &\mathbf{1}\left\{l_y(T_{i+1}) = \Lambda_y\left(l_y(T_i), \Phi(T_i), r(T_i), T_{i+1}, T_i\right)\right\} \\ &\mathbf{1}\left\{\Phi(T_{i+1}) = \Psi\left(\Phi(T_i), r(T_i), T_{i+1}, T_i\right)\right\} \\ &f\left(\frac{1}{r}(T_{i+1}), \tau(T_{i+1})|l_x(T_i), l_y(T_i), \Phi(T_i), \frac{1}{r}(T_i), \tau(T_i)\right). \end{aligned} \tag{18}$$

This is because $l_x(T_{i+1})$, $l_y(T_{i+1})$, and $\Phi(T_{i+1})$ are fully determined by $S(T_i)$ according to (15). Furthermore, since $1/r(T_{i+1})$ and $\tau(T_{i+1})$ are independently and identically distributed (i.i.d.) normal and exponential random variables selected at time T_{i+1}, they are independent from $S(T_i)$. Therefore, we can simplify (18) to

$$\begin{aligned} &f(S(T_{i+1})|S(T_i)) \\ &\quad = \mathbf{1}\left\{l_x(T_{i+1}) = \Lambda_x(l_x(T_i), \Phi(T_i), r(T_i), T_{i+1}, T_i)\right\} \\ &\mathbf{1}\left\{l_y(T_{i+1}) = \Lambda_y(l_y(T_i), \Phi(T_i), r(T_i), T_{i+1}, T_i)\right\} \\ &\mathbf{1}\left\{\Phi(T_{i+1}) = \Psi(\Phi(T_i), r(T_i), T_{i+1}, T_i) f\left(\frac{1}{r}(T_{i+1}), \tau(T_{i+1})\right)\right. \\ &\quad = \mathbf{1}\left\{l_x(T_{i+1}) = \Lambda_x\left(l_x(T_i), \Phi(T_i), r(T_i), T_{i+1}, T_i\right)\right\} \\ &\mathbf{1}\left\{l_y(T_{i+1}) = \Lambda_y\left(l_y(T_i), \Phi(T_i), r(T_i), T_{i+1}, T_i\right)\right\} \\ &\mathbf{1}\left\{\Phi(T_{i+1}) = \Psi\left(\Phi(T_i), r(T_i), T_{i+1}, T_i\right)\right\} \\ &\lambda e^{-\lambda\tau(T_{i+1})} \frac{1}{\sqrt{2\pi}\sigma} e^{-\frac{1}{2r^2(T_{i+1})\sigma^2}}. \end{aligned} \tag{19}$$

The Markov chain $S(T_i)$ is aperiodic, Φ-irreducible, and Harris recurrent, when λ and σ are finite and not equal to 0. Hence, there exists a unique invariant distribution measure, which is the stationary distribution [29]. Let us prove that the invariant distribution takes the following form:

$$\lim_{i\to\infty} f(S(T_i)) = \frac{1}{L}\frac{1}{W}\frac{1}{2\pi}\lambda e^{-\lambda\tau(T_i)} \frac{1}{\sqrt{2\pi}\sigma} e^{-\frac{1}{2r^2(T_i)\sigma^2}}. \tag{20}$$

To prove it, we only need to show that $\lim_{i\to\infty} f(S(T_i))$, as demonstrated in (20), satisfies

$$\begin{aligned}&\lim_{i\to\infty} f(S(T_i))\\&\quad=\lim_{i\to\infty} f\left(S(T_{i+1})\right)\\&\quad=\lim_{i\to\infty}\int_{S(T_i)\in\Omega} f(S(T_i))\, f\left(S(T_{i+1})|S(T_i)\right) dS(T_i)\end{aligned}\tag{21}$$

where Ω is the sample space of $S(T_i)$. The first equality is straightforward as $\tau(T_i)$ and $\tau(T_{i+1})$ are i.i.d. random variables, and $r(T_i)$ and $r(T_{i+1})$ are also i.i.d. random variables.

To show the second equality in (21), we substitute (19) and (20) into the right side of (21). Noticing that $\int_{l_x(T_i)=0}^{W} \mathbf{1}\{l_x(T_{i+1}) = \Lambda_x(l_x(T_i), \Phi(T_i), r(T_i), T_{i+1}, T_i)\} dl_x(T_i) = 1$ according to Lemma 1 and that similar relationships hold for $l_y(T_i)$ and $\Phi(T_i)$, we obtain

$$\begin{aligned}&\int_{S(T_i)\in\Omega} f\left(S(T_i)\right) f\left(S(T_{i+1})|S(T_i)\right) dS(T_i)\\&\quad=\int_{S(T_i)\in\Omega} \mathbf{1}\left\{l_x(T_{i+1})=\Lambda_x\left(l_x(T_i),\Phi(T_i),r(T_i),T_{i+1},T_i\right)\right\}\\&\mathbf{1}\left\{l_y(T_{i+1})=\Lambda_y\left(l_y(T_i),\Phi(T_i),r(T_i),T_{i+1},T_i\right)\right\}\\&\mathbf{1}\left\{\Phi(T_{i+1})=\Psi\left(\Phi(T_i),r(T_i),T_{i+1},T_i\right)\right\}\lambda e^{-\lambda\tau(T_{i+1})}\\&\frac{1}{\sqrt{2\pi}\sigma}e^{-\frac{1}{2r^2(T_{i+1})\sigma^2}}\frac{1}{L}\frac{1}{W}\frac{1}{2\pi}\,\lambda e^{-\lambda\tau(T_i)}\\&\qquad\times\frac{1}{\sqrt{2\pi}\sigma}\,e^{-\frac{1}{2r^2(T_i)\sigma^2}} d\left(S\left(T_i\right)\right)\\&\quad=\frac{1}{L}\frac{1}{W}\frac{1}{2\pi}\lambda e^{-\lambda\tau(T_{i+1})}\frac{1}{\sqrt{2\pi}\sigma}\,e^{-\frac{1}{2r^2(T_{i+1})\sigma^2}}\\&\quad=f\left(S(T_{i+1})\right).\end{aligned}\tag{22}$$

Finally, let us find the limiting probability distribution of the Markov process $S(t)$. According to the Palm formula [4], [31], the limiting distribution can be found by conditioning upon the stationary distribution of $S(T_i)$, where $T_i \to \infty$. In particular

$$\begin{aligned}&\lim_{t\to\infty} f\left(S(t)\right)\\&\quad=\frac{1}{E^0\left[\tau(T_i)\right]}E^0\left[\int_{T_i}^{T_i+\tau(T_i)}\mathbf{1}(S(t))dt\right]\\&\quad=\lambda E^0\left[\int_{T_i}^{T_i+\tau(T_i)}\mathbf{1}(S(t))dt\right]\\&\quad=\lambda\int_{S(T_i)\in\Omega}\int_{t=T_i}^{T_i+\tau(T_i)} f\left(S(T_i)\right) f\left(S(t)|S(T_i)\right) dt dS(T_i)\end{aligned}\tag{23}$$

where E^0 represents the empirical average. As shown in (23), $E^0[\tau(T_i)] = 1/\lambda$ because $\tau(T_i)$ is independently exponentially distributed with a finite mean $1/\lambda$.

Furthermore, noticing that, when t is between T_i and $T_i + \tau(T_i)$, $f(S(t)|S(T_i))$ can be found in a similar way to obtain (19). Substituting the expression of $f(S(t)|S(T_i))$ and (20) into (23) and using the same reasoning that derives (22), we obtain

$$\begin{aligned}&\int_{S(T_i)\in\Omega}\int_{t=T_i}^{T_i+\tau(T_i)} f\left(S(T_i)\right) f\left(S(t)|S(T_i)\right) dt dS(T_i)\\&\quad=\frac{1}{L}\frac{1}{W}\frac{1}{2\pi}\lambda e^{-\lambda\tau(t)}\frac{1}{\sqrt{2\pi}\sigma}\,e^{-\frac{1}{2r^2(t)\sigma^2}}\\&\int_{\tau(T_i)=0}^{\infty}\int_{t=T_i}^{T_i+\tau(T_i)}\lambda e^{-\lambda\tau(T_i)}dt d\tau(T_i)\\&\quad=\frac{1}{L}\frac{1}{W}\frac{1}{2\pi}\,\lambda e^{-\lambda\tau(t)}\frac{1}{\sqrt{2\pi}\sigma}\,e^{-\frac{1}{2r^2(t)\sigma^2}}\\&\int_{\tau(T_i)=0}^{\infty}\tau(T_i)\,\lambda e^{-\lambda\tau(T_i)}d\tau(T_i)\\&\quad=\frac{1}{L}\frac{1}{W}\frac{1}{2\pi}\,\lambda e^{-\lambda\tau(t)}\frac{1}{\sqrt{2\pi}\sigma}\,e^{-\frac{1}{2r^2(t)\sigma^2}}\frac{1}{\lambda}.\end{aligned}\tag{24}$$

Substituting (24) to (23) leads to $\lim_{t\to\infty} f(S(t)) = (1/L)(1/W)(1/2\pi)\lambda e^{-\lambda\tau(t)}(1/(\sqrt{2\pi}\sigma))e^{-1/(2r^2(t)\sigma^2)}$. Integrating with respect to $\tau(t)$ and $1/(r(t))$, we obtain that $f(l_x(t), l_y(t), \Phi(t)) = (1/L)(1/W)(1/2\pi)$ as $t \to \infty$. The proof is complete.

Theorems 1 and 2 demonstrate the uniform distribution of node locations and heading angles. The results also suggest the close analogy between the ST and RD models. Imposing the smooth trajectory requirement in the ST mobility model does not change the stationary uniform distribution of the RD model. This is because the wrap-around model avoids boundary impact, which is a key reason for nonuniform node distribution.

A Monte Carlo simulation of the node distribution is shown in Fig. 4(a). The simulation verifies the uniform node distribution proved in Theorem 2. In the simulation, an aerial vehicle is initially randomly placed in a 300×400 km^2 simulation area divided into grids of size 10×10 km^2. The vehicle then moves within the area, following the ST mobility model (with $V = 100$ m/s, $\sigma = 5 \times 10^{-5}$, $\Delta t = 1$ s, and $\lambda = 0.01/s$) and the wrap-around boundary model. The number of times that the vehicle falls in each grid is tracked. After sufficiently long simulation time, the counts are used to produce the node distribution at a steady state. We note that the uniform distribution also applies to the reflection boundary model, as shown in Fig. 4(b). The proofs can be easily adapted from the proofs for Theorems 1 and 2, by noticing the equivalence between these two boundary models [31]. The results also hold for the circular area [see simulations in Fig. 4(c) and (d)].

The uniform stationary node distribution directly leads to a series of network connectivity results, such as the distribution

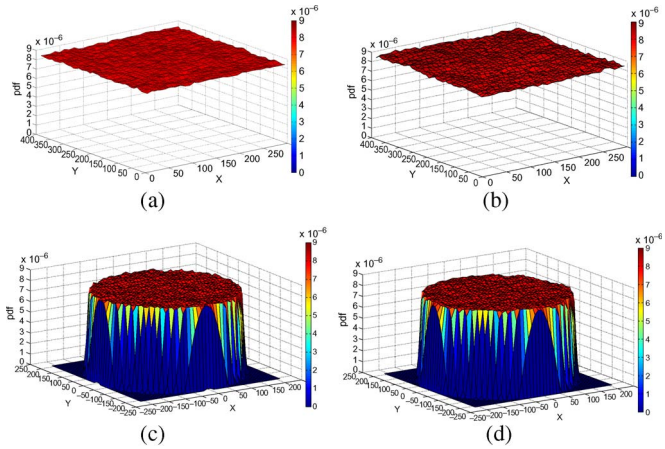

Fig. 4. Simulation of node distribution with (a) wrap-around model in a rectangular region, (b) reflection model in a rectangular region, (c) wrap-around model in a circular region, and (d) reflection model in a circular region.

of the number of neighbors for an individual node, the expected number of neighbors, the probability for a network to be connected, the probability for a network to be k-connected, and the transition range and number of neighbors required for the network to be connected with probability 1. See [7], [15], and [46] for details.

IV. Exploring Randomness

We envision that the *randomness/predictability* of mobility models is a crucial factor for the design of effective routing schemes but has not received much attention in the literature (see [6] for a very brief discussion). If a mobility model captures some degree of *predictability* for future trajectories, routing design could be significantly more effective by smartly taking into account this information. At one extreme, the routing design is fairly simple for a network of agents with deterministic trajectories. As relative locations of agents at future times are available beforehand to each agent, global optimization can be enacted to find the best routing design. At the other extreme, in completely random networks without any predictive information about future movement, it is highly possible that a relay node located at the boundary of transmission range (selected by the routing algorithms to minimize the number of hops) is moving out of the transmission range, leading to the loss of data transmission. To the best of our knowledge, there have been no quantitative studies on capturing the degree of randomness/predictability for mobility models. Here, we provide an *entropy*-based randomness measure for mobility models. As the focus of this paper is on modeling, we leave the utilization of randomness/predictability in robust routing design to the future work.

Another motivation to the study of randomness is concerned with better understanding of the existing AN mobility models. We observe that the three AN mobility models suitable for different applications are also aligned with different degrees of randomness. For instance, mobility patterns of UAVs for security and patrol purposes (captured by the ST mobility model) may be highly random. However, the ST model may be more deterministic than the RD model because it captures the spatiotemporal correlation of movement. UAVs used for search-and-rescue purposes (captured by the semi-random circular movement (SRCM) mobility model) are usually provided with certain target location information to start with; hence, their mobility patterns are less random. Commercial aircraft and UAVs envisioned for next-generation cargo transportation have preplanned trajectory information; hence, their mobility patterns (captured by the FP mobility model) are almost deterministic. Because of the significance of mobility models in routing design, there is a need to understand and differentiate the various AN mobility models in great depth and explore routing strategies to enhance network connectivity in each model. Randomness/predictability provides a measure for this kind investigation.

A. Definition of Randomness/Predictability

A natural metric for randomness is the entropy measuring the predictability of future trajectory conditioned upon the current information. We note that the entropy defined on a long look-ahead time does not help. For instance, RD, ST, and the SRCM mobility models all result in a uniform stationary node distribution, which does not differentiate among them. Therefore, we are motivated to study an *immediate* entropy measure defined at a very short time frame, using a Markov chain that describes the trajectory dynamics.

Specifically, the state of the Markov chain represents the vehicle status, such as position and direction. Randomness is defined based upon the entropy rate H [14]: $H = -\int_i \int_j p_i Q_{ij} \ln Q_{ij}$, where p_i is the probability to stay at state i, and Q_{ij} denotes the transition probability from state i to state j.

As a special case, if the states are uniformly distributed (e.g., when $t \to \infty$ for the RD and ST mobility models) and therefore p_i are all equal, and the pattern of the transition probabilities Q_{ij} associated with different state i is the same, the calculation of H can be simplified to $H' = -\int_j Q_{ij} \ln Q_{ij}$ for any i.

To facilitate the analysis, we consider a discretization of time and assume that the transition from one state to the other takes a unit time Δt, where Δt is sufficiently small.

B. Comparison of Randomness for AN Mobility Models

Here, we estimate the degree of randomness for four mobility models, including RD, SRCM, ST, and FP, using the entropy-rate-based metric. The quantitative analysis also allows us to evaluate the impact of model parameters on randomness and compare the four different mobility models. For a fair comparison, we assume that every model takes the same fixed forward speed V, and we ignore boundary effects.

1) RD Mobility Model: Assume that a vehicle keeps its direction for an exponentially distributed duration (with mean $1/\lambda$) before choosing its new direction uniformly distributed between 0 and 2π. Because of the uniform stationary distribution and the memoryless property, we can use the simplified randomness measure H'. Without loss of generality, assuming that the vehicle is moving from location 0 to the right, let us examine the probability of location and direction at time Δt. The

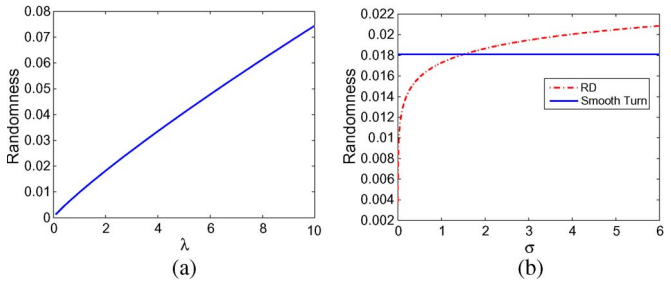

Fig. 5. (a) Randomness against λ in the RD model ($\Delta t = 0.001$ s). (b) Comparison of the randomness between the RD and ST mobility models ($\Delta t = 0.001$ s and $\lambda = 2/s$).

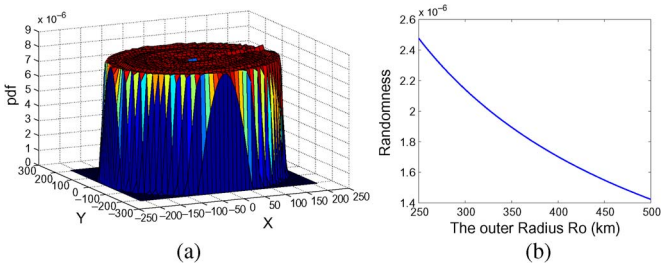

Fig. 6. (a) Uniform distribution of the SRCM model. (b) Degree of randomness decreases with the increase in the outer radius R_O ($\Delta t = 0.001$ s, $V = 40$ m/s, and $R_I = 100$ m).

probability of changing direction k times within Δt thus follows the Poisson distribution $P(n = k) = ((\lambda\Delta t)^k e^{-\lambda\Delta t})/k!$. As Δt is sufficiently small, we assume that the change of direction occurs at most once within Δt. Therefore, $P(n = 1) \approx \lambda\Delta t$, and $P(n = 0) \approx 1 - \lambda\Delta t$. If $n = 0$, the vehicle moves to the right and ends up at the location $V\Delta t$ with direction to the right. If $n = 1$, we assume that the change of direction occurs at the very beginning as Δt is very small. In this simplified case, the vehicle will locate uniformly on a circle centered at the starting location with heading directions pointing outward. As the direction is completely correlated with the location at Δt, we can find the probability associated with the ending location/direction as $1/(2\pi)$. Therefore, we can compute the randomness as

$$\begin{aligned} H_{RD} =& -P(n=0)\ln P(n=0) \\ & - \int_{\Phi=0}^{2\pi} \frac{P(n=1)}{2\pi} \ln \frac{P(n=1)}{2\pi} d\Phi \\ =& -(1-\lambda\Delta t)\ln(1-\lambda\Delta t) - \int_{\Phi=0}^{2\pi} \frac{\lambda\Delta t}{2\pi} \ln \frac{\lambda\Delta t}{2\pi} d\Phi \\ =& -(1-\lambda\Delta t)\ln(1-\lambda\Delta t) - \lambda\Delta t \ln \frac{\lambda\Delta t}{2\pi}. \end{aligned} \quad (25)$$

Interestingly, the speed of a vehicle does not affect the randomness of the model. Moreover, the degree of randomness increases with the increase in the parameter λ, as suggested in Fig. 5(a). This result is reasonable as λ represents how frequently a RD is selected. The more frequently an RD is selected, the more random the future trajectory becomes.

2) ST Mobility Model: As defined earlier in this paper, the basic ST mobility model assumes that a vehicle circles around for an exponentially distributed duration with mean λ before selecting a new turning radius with its inverse that is normally distributed with mean 0 and variance σ^2. Similar to the RD model, if no change in the turning center occurs within Δt, the vehicle will travel around its original turning center for a duration Δt. Otherwise, the vehicle will end up at a random location/heading direction by following a curve with the inverse of its turning radius r that is normally distributed with probability $e^{-1/2r^2\sigma^2}/(\sqrt{2\pi}\sigma)$. We thus can find the randomness for the ST model, in a way similar to that of the RD model, as follows:

$$\begin{aligned} H_{\mathrm{SR}} =& -P(n=0)\ln P(n=0) \\ & - \int_{\frac{1}{r}=-\infty}^{\infty} \frac{P(n=1)e^{-\frac{1}{2r^2\sigma^2}}}{\sqrt{2\pi}\sigma} \ln \frac{P(n=1)e^{-\frac{1}{2r^2\sigma^2}}}{\sqrt{2\pi}\sigma} d\frac{1}{r} \\ =& -(1-\lambda\Delta t)\ln(1-\lambda\Delta t) \\ & - \int_{\frac{1}{r}=-\infty}^{\infty} \frac{\lambda\Delta t e^{-\frac{1}{2r^2\sigma^2}}}{\sqrt{2\pi}\sigma} \ln \frac{\lambda\Delta t e^{-\frac{1}{2r^2\sigma^2}}}{\sqrt{2\pi}\sigma} d\frac{1}{r} \\ =& -(1-\lambda\Delta t)\ln(1-\lambda\Delta t) - \lambda\Delta t \ln \frac{\lambda\Delta t}{\sqrt{2\pi e}\sigma}. \end{aligned} \quad (26)$$

The result suggests that V does not also impact the randomness of the ST mobility model. However, both λ and σ play a role in the degree of randomness. In particular, the randomness is less with smaller σ, which suggests more straight trajectory. For large σ, denoting high variability of turning radius, the location and direction of the vehicle can be very uncertain. In summary, the randomness of the ST mobility model is less than that of the RD model when σ is less than a threshold. The comparison between (25) and (26) suggests that threshold $\sigma = (2\pi)/e$ [see also Fig. 5(b)].

3) SRCM Mobility Model: We consider an SRCM model that is slightly different from the one described in [44]. Again, we assume a constant forward speed V and a fixed center. Upon the completion of one round, the vehicle chooses radius r that is *uniformly* distributed between r_I and r_O (where $V\Delta t \ll r_I < r_O$). We also assume that the transition time from one radius to the other is neglected, and we only consider the circular movement, as suggested in [44]. The resulting node distribution is uniform, as shown in Fig. 6(a). We note that the analysis of randomness for the SRCM model is different from that of the RD and ST models, in the sense that the original randomness measure H needs to be used, instead of the simplified H'. This is because the SRCM model does not have the memoryless property; as such, the distance that the vehicle has traveled along a circle is of importance. Hence, the pattern of Q_{ij} is different for different i. In a small time interval Δt, if the vehicle has traveled along a circle with radius r for a distance less than $2\pi r$, the vehicle will continue moving along the circle with probability $Q_{ij} = 1$; otherwise, the vehicle will end up at

Mobility Model	RD	ST	SRCM	FP
Application	MANET	Patrolling	Search and rescue	Cargo and commercial
Degree of Randomness	Highest	Medium	Low	Lowest

Fig. 7. Comparison of randomness among the four mobility models.

a circle with the radius uniformly distributed with probability $Q_{ij} = 1/(r_O - r_I)$.

To facilitate the analysis, we first obtain the entropy rate conditioned upon the current radius r and then integrate over all possible radii. As the randomness associated with any radius r only occurs when the vehicle changes its radius within Δt (with probability $V\Delta t/(2\pi r)$), we find $H_{\rm SC}|r = -(V\Delta t/(2\pi r))\int_{r=r_I}^{r=r_O} 1/(r_O - r_I)\ln 1/(r_O - r_I)dr = -V\Delta t/(2\pi r)\ln 1/(r_O - r_I)$. Integrating over the range of r, we obtain

$$\begin{aligned} H_{\rm SC} &= \int_{r=r_i}^{r=r_O} -\frac{V\Delta t}{2\pi r}\ln\frac{1}{r_O - r_i}\frac{1}{r_O - r_i}dr \\ &= -\frac{1}{r_O - r_i}\ln\frac{1}{r_O - r_i}\frac{V\Delta t}{2\pi}\int_{r=r_i}^{r=r_O}\frac{1}{r}dr \\ &= -\frac{1}{r_O - r_i}\ln\frac{1}{r_O - r_i}\frac{V\Delta t}{2\pi}(\ln r_O - \ln r_i). \quad (27) \end{aligned}$$

In the ST mobility model, both the velocity V and the area defined by the radii R_O and R_I affect the randomness. Clearly, the degree of randomness proportionally increases with the increase in V; however, it typically decreases with the increase in R_O [as shown in Fig. 6(b)]. It is also observed that, under typical maneuvering conditions, the randomness of the ST model is larger than that of the SRCM model.

4) FP-Based Mobility Model: With the simplest assumption that a trajectory follows a preplanned trajectory with a tiny variation modeled by a Gaussian noise (with mean 0 and variance $\hat{\sigma}^2$), we have $H_{\rm FP} = \ln(\sqrt{2\pi e}\hat{\sigma})$. When $\hat{\sigma} < 1/(\sqrt{2\pi e})$, the entropy is negative, representing the randomness to be less than a uniform distribution in [0,1] [13].

In summary, the randomness and application categories of the RD model and three AN mobility models discussed here are listed in Fig. 7.

V. Variants of the ST Mobility Model

Finally, let us discuss possible variants and enhancements of the ST mobility model.

Enhanced Modeling of Model Parameters: This basic ST mobility model can be easily generalized to include varying forward speed and 3-D movement. In addition, as an airborne vehicle typically has a certain minimum safe turning radius, instead of roughly modeling $1/r$ as a Gaussian variable, we can provide a more detailed model for r and require r to reside in the safe range. All of the given enhancements maintain the uniform distribution of node locations and directions. We also note that the random model in [24] is a variant of the ST model, e.g., with the assumption that the radius r takes two fixed constants and ∞. An enhanced pheromone repel model that maximizes coverage is also introduced therein. Geographical routing is developed for this mobility model [23].

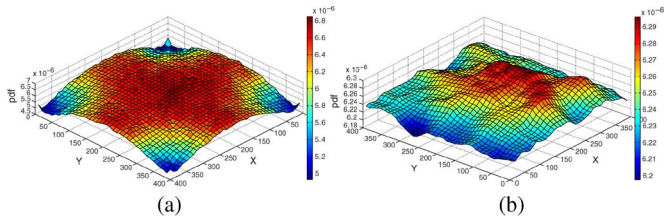

Fig. 8. Simulation of node distribution for (a) random-center RWP-alike ST mobility model and (b) for random-destination RWP-alike ST model after smoothening.

Collision Avoidance: In the current mobility model, we assume that each vehicle moves independently. In reality, neighboring airborne vehicles need to satisfy a safe separation distance; therefore, proper collision avoidance mechanisms may be included. As the centripetal and tangential accelerations are directly captured in the mobility model, control mechanisms for collision avoidance can be easily added (see [10] for a related implementation) if desired.

RWP-Like ST Mobility Model: The current ST mobility model resembles the RD model equipped with smooth trajectory. We can similarly develop RWP-like ST mobility models. Possible strategies include 1) randomly choosing a center, which satisfies the smooth trajectory requirement and is uniformly distributed in the region, and circling around it for an exponential duration, before choosing another center; and 2) randomly choosing a destination that is uniformly distributed in the region and reaching it along a smooth trajectory before choosing another destination. Similar to the RWP models, we also observe nonuniform node distributions (see Fig. 8).

VI. Concluding Remarks and Future Work

In this paper, we have presented a novel ST random mobility model for highly random ANs. The ST mobility model captures the tendency of airborne vehicles toward making straight trajectories and STs. It is developed based upon the physical laws and aerodynamic constraints governing moving aerial objects, whereas it is simple enough for tractable analysis. We prove that, similar to the RD model, the stationary node distribution is uniform. This result permits a series of closed-form connectivity properties.

Randomness is an important characteristic of mobility models in that 1) it is a natural metric to characterize mobility models, and 2) it serves as an important factor for the design/selection of robust routing algorithms. As such, we have developed a quantified randomness measure using the entropy rate. Then we compute and compare the degrees of randomness for four mobility models. Compared with the FP and SRCM mobility models, the ST model represents the highest degree of randomness, but is less random than RD because of the constraint on smooth trajectory specific to airborne vehicles. The ST mobility model can be viewed as an RD model equipped with smooth trajectory, with the only difference being

that it randomly chooses a turning radius instead of a heading direction. The classification of AN mobility models based upon the degree of randomness aligns with the classification based on applications. Different AN mobility models are needed for different applications (e.g., transportation, search-and-rescue, and patrolling) due to their diversity.

We will investigate various enhanced versions of the ST mobility model, as suggested in Section V, in the future. We will also fit model parameters using real UAV flight data for model validation. Moreover, we will investigate area coverage as the full coverage and the time needed are also important characteristics of ANs [28], [34]. Finally, we will have further investigation with more advanced connectivity properties, such as path duration and link duration, and we will fully investigate the impact of randomness on the performance of routing protocols and design effective routing protocols that utilize this information.

ACKNOWLEDGMENT

The authors would like to thank D. He for some preliminary study and the editor and anonymous reviewers for their suggestions to improve this paper.

REFERENCES

[1] [Online]. Available: http://ee.unt.edu/public/wan/SNDC.htm
[2] [Online]. Available: http://en.wikipedia.org/wiki/Triangle_wave
[3] *Instrument Flying Handbook*, U.S. Dept. Transp., Fed. Aviation Admin., Airman Testing Standards Branch, Oklahoma City, OK, USA, 2008.
[4] F. Baccelli and P. Brémaud, *Elements of Queuing Theory: Palm Martingale Calculus and Stochastic Recurrence*. Berlin, Germany: Springer-Verlag, 1994.
[5] F. Bai and A. Helmy, "A survey of mobility modeling and analysis in wireless ad hoc networks," in *Wireless Ad Hoc and Sensor Networks*. New York, NY, USA: Springer-Verlag, Oct. 2006.
[6] C. Bettstetter, "Smooth is better than sharp: A random mobility model for simulation of wireless networks," in *Proc. ACM Int. Workshop Model., Anal. Simul. Wiresless Mobile Syst.*, Rome, Italy, Jul. 2001, pp. 19–27.
[7] C. Bettstetter, "On the connectivity of ad hoc networks," *Comput. J.*, vol. 47, no. 4, pp. 432–447, 2004.
[8] C. Bettstetter, H. Hartenstein, and X. Pérez-Costa, "Stochastic properties of the random waypoint mobility model," *Wireless Netw.*, vol. 10, no. 5, pp. 555–567, Sep. 2004.
[9] K. Bilimoria, B. Sridhar, G. Chatterji, K. Sheth, and S. Grabbe, "FACET: Future ATM concepts evaluation tool," *Air Traffic Control Quart.*, vol. 9, no. 1, pp. 1–20, 2001.
[10] F. Borrelli, T. Keviczky, and G. J. Balas, "Collision-free uav formation flight using decentralized optimization and invariant sets," in *Proc. 43rd IEEE Conf. Decision Control*, Dec. 2004, pp. 1099–1104.
[11] J. Boudec and M. Vojnovic, "Perfect simulation and stationarity of a class of mobility models," EPFL, Lausanne, Switzerland, Tech. Rep. EPFL/IC/2004/59, Jul. 2004.
[12] Z. Cheng and W. B. Heinzelman, "Exploring long lifetime routing (LLR) in ad hoc networks," in *Proc. 7th ACM Int. Symp. Model. Anal. Simul. Wireless Mobile Syst.*, 2004, pp. 203–210.
[13] K. Conrad, Probability distributions and maximum entropy. [Online]. Available: http://www.math.uconn.edu/kconrad/blurbs/entropy.pdf
[14] L. Ekroot and T. M. Cover, "The entropy of Markov trajectories," *IEEE Trans. Inf. Theory*, vol. 39, no. 4, pp. 1418–1421, Jul. 1993.
[15] N. M. Freris, H. Kowshik, and P. R. Kumar, "Fundamentals of large sensor networks: Connectivity, capacity, clocks and computation," *Proc. IEEE*, vol. 98, no. 11, pp. 1828–1846, Nov. 2010.
[16] B. Fu and L. A. DaSilva, "A mesh in the sky: A routing protocol for airborne networks," in *Proc. IEEE Mil. Commun. Conf.*, Orlando, FL, USA, Oct. 2007, pp. 1–7.
[17] R. Ghanta and S. Suresh, "Influence of mobility models on the performance of routing protocols in ad-hoc wireless networks," in *Proc. IEEE 59th Veh. Technol. Conf.*, Milan, Italy, May 2004, vol. 4, pp. 2185–2189.
[18] B. Gloss, M. Scharf, and D. Neubauer, "A more realistic random direction mobility model," in *Proc. 4th Manage. Committee Meet.*, Würzburg, Germany, Oct. 2005, pp. 1–11.
[19] R. A. Guérin, "Channel occupancy time distribution in a cellular radio system," *IEEE Trans. Veh. Technol.*, vol. VT-36, no. 3, pp. 89–99, Aug. 1987.
[20] J. P. Helferty, "Improved tracking of maneuvering targets: The use of turn-rate distributions for acceleration modeling," in *Proc. IEEE Int. Conf. Multisens. Fusion Integr. Intell. Syst.*, Las Vegas, NV, USA, Oct. 1994, pp. 515–520.
[21] D. Hong and S. S. Rappaport, "Traffic model and performance analysis for cellular mobile radio telephone systems with prioritized and nonprioritized handoff procedures," *IEEE Trans. Veh. Technol.*, vol. VT-35, no. 3, pp. 77–92, Aug. 1986.
[22] E. Hyytiä, P. Lassila, and J. Virtamo, "Spatial node distribution of the random waypoint mobility model with applications," *IEEE Trans. Mobile Comput.*, vol. 5, no. 6, pp. 680–694, Jun. 2006.
[23] E. Kuiper and S. Nadjm-Tehrani, "Mobility models for uav group reconnaissance applications," in *Proc. Int. Conf. Wireless Mobile Commun.*, Bucharest, Romania, Jul. 2006, p. 33.
[24] E. Kuiper and S. Nadjm-Tehrani, "Geographical routing with location service in intermittently connected MANETs," *IEEE Trans. Veh. Technol.*, vol. 60, no. 2, pp. 592–604, Feb. 2011.
[25] X. R. Li and V. P. Jilkov, "A survey of maneuvering target tracking: Dynamic models," in *Proc. SPIE Conf. Signal Data Process. Small Targets*, Orlando, FL, USA, Apr. 2000, vol. 4048, pp. 212–235.
[26] B. Liang and Z. J. Haas, "Predictive distance-based mobility management for multidimensional pcs networks," *IEEE/ACM Trans. Netw.*, vol. 11, no. 5, pp. 718–732, Oct. 2003.
[27] G. Lim, K. Shin, S. Lee, H. Yoon, and J. Ma, "Link stability and route lifetime in ad-hoc wireless networks," in *Proc. Int. Conf. Parallel Process. Workshops*, Vancouver, BC, Canada, Aug. 2002, pp. 116–123.
[28] B. Liu, O. Dousse, P. Nain, and D. Towsley, "Dynamic coverage of mobile sensor networks," *IEEE Trans. Parallel Distrib. Syst.*, vol. 24, no. 2, pp. 301–311, Feb. 2013.
[29] S. P. Meyn and R. L. Tweedieé, *Markov Chains and Stochastic Stability*. London, U.K.: Springer-Verlag, 1993.
[30] N. Nabaa and R. H. Bishop, "Validation and comparison of coordinated turn aircraft maneuver models," *IEEE Trans. Aerosp. Electron. Syst.*, vol. 36, no. 1, pp. 250–259, Jan. 2000.
[31] P. Nain, D. Towsley, B. Liu, and Z. Liu, "Properties of random direction models," in *Proc. 24th Annu. Joint Conf. IEEE Comput. Commun. Soc.*, Mar. 2005, pp. 1897–1907.
[32] H. Narra, E. K. Çetinkaya, and J. P. Sterbenz, "Performance analysis of aerorp with ground station advertisements," in *Proc. 1st ACM Airborne*, 2012, pp. 43–47.
[33] A. Papoulis and S. U. Pillaié, *Probability, Random Variables and Stochastic Processes*. New York, NY, USA: McGraw-Hill, 2002.
[34] Y. Peres, A. Sinclair, P. Sousi, and A. Stauffer, "Mobile geometric graphs: Detection, coverage and percolation," in *Proc. SODA*, San Francisco, CA, USA, Jan. 2011, pp. 412–428.
[35] K. Peters, A. Jabbar, E. Cetinkaya, and J. Sterbenz, "A geographical routing protocol for highly-dynamic aeronautical networks," in *Proc. IEEE WCNC*, Cancun, Mexico, Mar. 2011, pp. 492–497.
[36] J. P. Rohrer, E. K. Cetinkaya, H. Narra, D. Broyles, K. Peters, and J. P. G. Sterbenz, "Aerorp performance in highly-dynamic airborne networks using 3D gauss-Markov mobility model," in *Proc. Military Commun. Conf.*, Baltimore, MD, USA, Nov. 2011, pp. 834–841.
[37] J. Rohrer, A. Jabbar, E. Cetinkaya, E. Perrins, and J. Sterbenz, "Highly-dynamic cross-layered aeronautical network architecture," *IEEE Trans. Aerosp. Electron. Syst.*, vol. 47, no. 4, pp. 2742–2765, Oct. 2011.
[38] K. Sampigethaya, R. Poovendran, S. Shetty, T. Davis, and C. Royalty, "Future e-enabled aircraft communications and security: The next 20 years and beyond," *Proc. IEEE*, vol. 99, no. 11, pp. 2040–2055, Nov. 2011.
[39] R. A. Singer, "Estimating optimal tracking filter performance for manned maneuvering targets," *IEEE Trans. Aerosp. Electron. Syst.*, vol. AES-6, no. 4, pp. 473–483, Jul. 1970.
[40] A. Tiwari, A. Ganguli, A. Sampath, D. Anderson, B. H. Shen, N. Krishnamurthi, J. Yadegar, M. Gerla, and K. David, "Mobility aware routing for the airborne network backbone," in *Proc. Military Commun. Conf.*, San Diego, CA, USA, Nov. 2008, pp. 1–7.
[41] Y. Wan, K. Namuduri, Y. Zhou, D. He, and S. Fu, "A smooth-turn mobility model for airborne networks," in *Proc. 1st ACM MobiHoc Workshop Airborne Netw. Commun.*, Hilton Head, SC, USA, Jun. 2012, pp. 25–30.
[42] Y. Wan and S. Roy, "A scalable methodology for evaluating and designing coordinated air traffic flow management strategies under uncertainty," *IEEE Trans. Intell. Transp. Syst.*, vol. 9, no. 4, pp. 644–656, Dec. 2008.

[43] Y. Wan and S. Roy, "Uncertainty evaluation through mapping identification in intensive dynamic simulations," *IEEE Trans. Syst., Man, Cybern. A, Syst., Humans*, vol. 40, no. 5, pp. 1094–1104, Sep. 2010.
[44] W. Wang, X. Guan, B. Wang, and Y. Wang, "A novel mobility model based on semi-random circular movement in mobile ad hoc networks," *Inf. Sci.*, vol. 180, no. 3, pp. 399–413, Feb. 2010.
[45] L. A. Wojcik, F. A. Amodeo, D. N. Buza, J. A. Nardelli, and F. P. Wieland, "World regional air traffic modeling with DPAT," MITRE, McLean, VA, USA, Tech. Rep. MTR-97W00 000 070, 1997.
[46] F. Xue and P. R. Kumar, "The number of neighbors needed for connectivity of wireless networks," *Wireless Netw.*, vol. 10, no. 2, pp. 169–181, Mar. 2004.

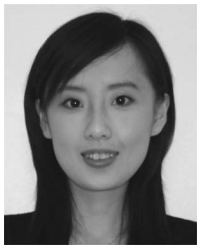

Yan Wan (S'08–M'09) received the B.S. degree from Nanjing University of Aeronautics and Astronautics, Nanjing, China, in 2001; the M.S. degree from The University of Alabama, Tuscaloosa, AL, USA, in 2004; and the Ph.D. degree from Washington State University, Pullman, WA, USA, in 2009.

She worked as a Postdoctoral Scholar with the control systems program, University of California, Santa Barbara, CA, USA. She is currently an Assistant Professor with the Department of Electrical Engineering, University of North Texas, Denton, TX, USA. Her research interests include decision-making tasks in large-scale networks, with applications to air traffic management, sensor networking, biological systems, etc.

Dr. Wan received the prestigious William E. Jackson Award (excellence in aviation electronics and communication) from the Radio Technical Commission for Aeronautics in 2009.

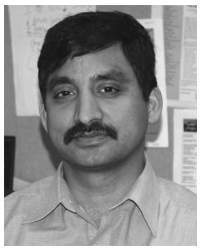

Kamesh Namuduri (SM'97) received the B.S. degree in electronics and communication engineering from Osmania University, Hyderabad, India, in 1984; the M.S. degree in computer science from the University of Hyderabad, in 1986; and the Ph.D. degree in computer science and engineering from the University of South Florida, Tampa, FL, USA, in 1992.

From 1984 to 1986, he worked with the Centre for Development of Telematics, which is a telecommunications firm in India, where he participated in the development of the first indigenous digital exchange in India. From 1993 to 1997, he worked with GTE Telecommunication Services Inc. (now Verizon), where he participated in the development of a mobile telephone fraud-detection system. From 1998 to 2002, he worked as a Research Scientist with the Center for Theoretical Studies of Physical Systems, Clark Atlanta University, Atlanta, GA, USA. From 2002 to 2008, he was a faculty member with the Department of Electrical Engineering and Computer Science, Wichita State University, Wichita, KS, USA. He is currently with the Department of Electrical Engineering, University of North Texas, Denton, TX, USA, as an Associate Professor. His research interests include information security, image/video processing and communications, and ad hoc sensor networks.

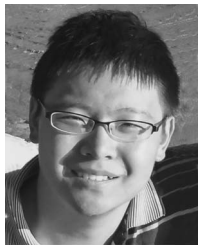

Yi Zhou (S'11) was born in Nanjing, China, in 1985. He received the B.S. degree from Jiang Su University, Zhenjiang, China, in 2007 and the M.S. degree from the University of North Texas, Denton, TX, USA, in 2011. He is currently working toward the Ph.D. degree with the Department of Electrical Engineering, University of North Texas.

His research interests include stochastic modeling, queuing theory, and air traffic flow management.

Shengli Fu (S'03–M'05–SM'08) received the B.S. and M.S. degrees in telecommunication engineering from Beijing University of Posts and Telecommunications, Beijing, China, in 1994 and 1997, respectively; the M.S. degree in computer engineering from Wright State University, Dayton, OH, USA, in 2002; and the Ph.D. degree in electrical engineering from the University of Delaware, Newark, DE, USA, in 2005.

He is currently an Associate Professor with the Department of Electrical Engineering, University of North Texas, Denton, TX, USA. His research interests include coding and information theory, wireless communications and sensor networks, and mobile ad hoc networks.